

UNIVERSITY OF DEBRECEN
Centre of Agricultural Sciences
Faculty of Agricultural Sciences
Department of Machinery

**INTERDISCIPLINARY AGRICULTURAL SCIENCES
DOCTORAL SCHOOL**

Head of Doctoral School:
Prof. dr. János Nagy
doctor of HAS

Consultant:
Dr. Zoltán Csizmazia
Ph.D.

DOCTORAL (Ph.D.) THESIS

**PHYSICAL PROPERTIES OF FERTILIZER PARTICLES AND THEIR
MOVEMENT ANALYSIS**

Prepared by:
Ágnes Battáné Gindert-Kele

Debrecen
2005

1. OBJECTIVES OF THE RESEARCH, INTRODUCTION

Plants ensure their development by nutrients gained from the soil and atmosphere. Nutrients supplied during agricultural production are often fertilizers. Economical, efficient and even precise spreading of nutrients can be realised only by properly designed machines. Nearly 90% of the 140 million tons of annual fertilizer production is spread with spinning disc machines. The physical properties of different fertilizers are significantly variable, which affects essentially their distribution to the cultivation area. In the progress of machine development the trajectories of discharging particles should be calculated in order to get the spreading pattern on the soil.

Leaving the spinning-device, the initial kinetic condition of the particle and the air drag forces determine the path of flying particles. Practice requires the estimation the ballistic curve with reasonable accuracy. For nearly spherical particles the tangential drag is considered proportional to the square number of velocity. However, in the case of irregular particles the alternation of the drag on the path results in stray of particle impact points. One of the essential theoretical points of this thesis is whether the trajectories calculated from the measured air-drag coefficients are accurate enough if compared to practical results. Approximations of the calculations are necessary since our knowledge on experimental conditions is limited, and on the other hand, too complicated theoretical descriptions can be tractable.

My Research Aims:

- To elaborate a simulation program (called “virtual fertilizer spreader”) by which – knowing the physical properties and initial velocities and discharge angles of particles – it executes ballistic calculations and predicts the spreading pattern behind the spreader with a close approximation.
- I have determined a numerous geometric and physical properties of particles and its clusters of different commercial fertilizers by a number of measurements.
- On the one hand, for the measurements, I have used equipments available at the Department of Machinery, I altered or modified them as well as the measuring procedures based on my experience. On the other hand, I developed two new measuring devices for the Department of Machinery.

I have examined important physical characteristics of five different fertilizers used in our country, which affect the trajectory and influence the landing position of the discharging particles. I examined and analysed the size, shape, weight and density distribution, average

degree of humidity and porosity of sample particles and the particle aggregation. In order to determine the air-drag coefficient that we assume constant I made floating and sinking measurements in air and paraffin. To complete the list of physical parameters for use in future research I determined the drag factor approximating the drag coefficient by sliding measurements on ten different plane plates of different material and on the particle aggregation itself.

I estimated the initial kinematics values for simulating trajectories based on literature data and on data kindly provided by my colleagues. The movement analysis of the particles on the spinning disc for obtaining initial kinematics or execution of spreading experiments on the field were not among the goals of this work, though set up experiments for a given spreader and a fertilizer of unknown physical properties are invaluable. One of the applications of my trajectory simulations could be the determination of initial kinetic conditions - depending on fertilizer type - for the requested spreading pattern. Based on it, one can suggest modifications of the constructions, which can be put to good use by machine designers. Simulations reduce experimental expenses, allow interpolation between measured figures with acceptable accuracy, thereby the distribution of fertilizers may become more economical. On this basis, manufacturers can provide useful charts for the user that ensures the proper use of the spreader.

2. BACKGROUND OF MY RESEARCH

At the Department of Machinery, there have been extensive studies for decades concerning fertilizer distribution with Professor Zoltán Csizmazia in charge. The research is up-to-date since high area performance is possible by spinning disc fertilizer distributors spread all over the world. Not surprisingly, their improvement is on the agenda. Olieslagers¹ compared the calculated spreading pattern of his theoretical model with the measurements using the same spinning disc construction. However, theoretical and practical results were significantly different. Moshou et al.² chose a way that is more practical: they proved that pictures of spreading are predictable with “neural network” algorithms if they process the settings of spreaders and physical properties of fertilizers in a learning procedure. To replace spreading

¹ OLIESLAGERS, R., RAMON, H. & DEBAERDEMAEKER, J. (1996). *Journal of Agricultural Engineering Research* **63**, 137-152.

² MOSHOU, D., DEPREZ, K. & RAMON, H. (2004). *Mathematics and Computers in Simulation* **65**, 77-85.

experiments in measuring halls Reumers³ et al. introduced a small 'in situ' collection device for obtaining cylindrical and tangential distribution of the particles. Grift et al.⁴ tried 'online' measuring the properties of particles leaving the disc. This way the expected picture of spreading can be estimated immediately by ballistic calculation, which allows us to control the settings of fertilizer spreader 'online'. The new principle: 'rather calculate than collect' is adjusted to the needs of precision agriculture, allows cost saving experiments and in the long run it can lead to developing new generation of fertilizer spreaders. One could regard my thesis as an initial step towards this direction.

3. MATERIAL AND METHOD OF INVESTIGATIONS

I made the measurements and experiments in the Materials Testing Laboratory of Department of Machinery at University of Debrecen, Centre of Agricultural Sciences, Faculty of Agricultural Sciences at temperature of 20°C and 30-40% relative humidity. Fifty kg of the following types of fertilizers was available in hermetic bags:

1. Urea (46-0-0, Nitrogénművek Rt. Pétfürdő)
2. Ammonium nitrate (34% N, Nitrogénművek Rt. Pétfürdő)
3. Granulated Potassium (0-0-60%, Tiszamenti Vegyiművek Rt. Szolnok)
4. NPK 15-15-15 (Agrolinz Agrochemikalien GmbH)
5. Salt of Linz (mészammonsalétrom 27% N, Agrolinz Melamin GmbH).

Measuring the properties of particle clusters

In order to determine *humidity* of fertilizers I heated three times repeatedly 25 grams of fertilizers each for four hours at temperature of $103 \pm 1^\circ\text{C}$ in drying-oven. The humidity was calculated from the weight before and after drying. For *classification with screen*, I took three different, independent 500-500 grams of samples for each type and treated them for 3 minutes with shaking machine. The applied screen size was 0.8 mm, 1 mm, 2 mm, 2.5 mm, 4 mm and 6.3 mm.

To determine *bulk density* (ρ_b) I used 1000 cm³ measuring tank. The '*real*' density of the solid material (ρ_s) was determined in three ways:

³ REUMERS, J., TIJSKENS, E. & RAMON, H. (2003). *Biosystems Engineering* **86**, 431-439.

⁴ GRIFT, T. E. & HOFSTEE, J. W. (2002). *Transactions of the Asae* **45**, 561-567.

- with liquid picnometer using ~ 1 – 5 grams of samples
- with air picnometer using ~ 150-200 grams of samples
- with paraffin displacement in graduated cylinder on fertilizer sample that has already been measured with air picnometer (~150-200 grams of samples)

I filled the liquid picnometer of 10 ml capacity up with paraffin. The volume of particles was determined based on the weight and density of paraffin displaced by the particles, then the average density of the fertilizer was calculated from the weight of particles. I defined the density ρ_s of fertilizers with the help of air picnometer method as well. Since I developed this tool, the description of this instrument can be read among the results (vide infra, 3.1). As a control, I determined the density of samples measured by air picnometer also with liquid displacement method, in a graduated cylinder filled with paraffin. I applied the equation $\Phi_t = 1 - \rho_b / \rho_s$ to specify the total *porosity* Φ_t of the fertilizers tested.

Appliances and methods suitable for examination of frictional properties

I specified the frictional properties of fertilizer particles using the sliding appliance previously developed at the Department of Machinery. Particle movement on the vanes of spinning discs may be single or multi-layer. Our sliding equipments model rather the latter. For an average lone particle on a usual disc the maximal force acting on a particle is not bigger than 0.1-0.2 N as estimated using the appropriate dynamics equation. When the sliding appliance is differently loaded, the normal force acting at one particle changes in the 0.01-0.3 N range (for the given 200x200 mm plate, with 25-750 N load and an estimated particle number). Hence, the sliding factor is measured under conditions similar to everyday spreading work. Sliding velocity was constant, 4.6 mm/s on a 50 mm path.

Sliding of fertilizers were tested on the following surfaces: stainless steel, black steel, galvanized steel sheet, aluminium, teflon-coated steel sheet, bakelite, PVC, Plexiglas, glass and laminated wood. To determine inner friction I used a ‘rotary sliding-equipment’. In the case of each fertilizer and surface, I started measurements by specifying the idle force and used six different loading per measurements. I tested samples of fertilizers in thin layer to achieve life-like frictional properties.

The natural dynamic repose of fertilizer aggregations were determined with measuring box, by removing it’s front wall with the exception of a 100 mm long part. I filled the box with the tested fertilizer, and then I removed the front wall suddenly but without any percussion. Inner friction can be calculated from the dynamic angle of repose with the equation $\mu = \text{tg } \alpha = a/b$

where 'a' is the level of fertilizer measured above the outlet hole of the box, and $b = 300\text{mm}$ is the size of the box perpendicular to the outlet hole.

Physical properties measured per particle

Size, shape, mass and density

I chose samples with 250 elements with random sampling for each type of fertilizers in order to determine size and mass of particles. For the geometric description of the particles I measured their longest dimension (d_1) and the values measured along the two axis perpendicular to it (d_2, d_3) with 0.01mm precision digital calliper gauge. I used 0.1mg precision scales to measure the mass of particles. Specification of a particle's 'ball-shape' number took place based on the proportion of the geometric middle diameter and d_1 : $g_a = (d_1 d_2 d_3)^{1/3} / d_1$. I calculated the approximate values of density for each particle ρ_{szi} with the assumption that the volume of particles is in proportion to the conjunction of the three perpendicular dimensions, and density calculated from the mass and volume sum of the measured particles' cluster must be in accordance with the real ρ_s density of the fertilizer. Visual inspection of particles shows that potash crystals have irregular, crystal shapes while the other brands exhibit spherical shape similar to droplets; their consistence is protected by coat. Particle aggregation or dust are negligible for fresh samples.

Measuring aerodynamic properties

For the measurement of the air-resistance coefficient I applied a vertical *air channel* (elutriator)⁵. The velocity of the airflow was measured with a thermal sphere anemometer. In the air channel, I measured the floating velocity of each particle in the samples of 250 particles. I developed a descent pipe filled with paraffin to determine the aerodynamic properties of the particles in a simple, alternative way.

3.1. Instrument developments

3.1.1. Development and application of an air picnometer for measuring density of fertilizers

Real volume of bodies with cavities can be measured with air picnometers as the air can freely enter the inclusions. The parts of the symmetrically built dry picnometer (**Fig. 1**) are the two

⁵ CSIZMAZIA, Z., LAJOS, T., MARSHALL, J. & POLYÁK, N. I. (2000). *Mezőgazdasági Technika*, 2-5.

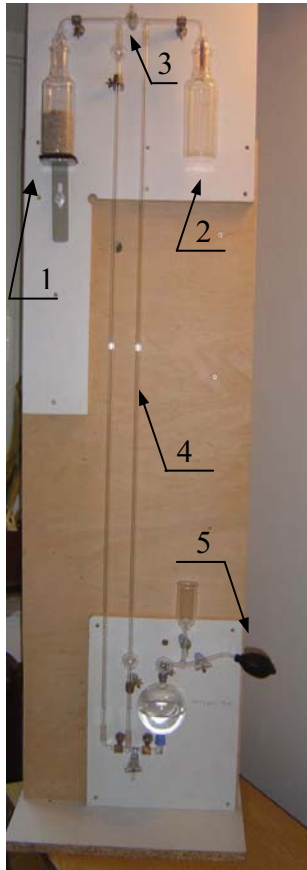


Figure 1. Air-pycnometer

measuring tanks(1, 2) with identical capacity, the valve (3) placed in the pipe linking the two chambers and the differential manometer (4) joining them. At the beginning of measurement, the liquid column in the two vertical stems of the manometer starts from the same bottom level, at atmospheric pressure. After closing the cocks, we increase the air pressure in the two measuring chambers with hand pumps (5). According to my calculations during air pycnometer measurement it is not necessary to bring the liquid levels to the same level because the calibration method I suggest allows accurate volume measuring at any manometer setting as well. This finding makes the application of air pycnometer easier compared to the earlier procedures.

After calibrating the instrument, I made the measurements with three repetitions on five different types of fertilizers. To check the density values specified with the pycnometer (ρ_{lp}) I also applied the method of liquid-displacement on the same samples.

3.1.2. Development of liquid descent pipe measuring instrument

Measurement of air drag coefficient of irregularly shaped fertilizer particles can usually be done in a vertical air channel or by dropping in large descent pipes. More accurate and simpler measurement is possible with the descent pipe filled with paraffin. The descent pipe that I designed (**Fig. 2.**) is a transparent glass pipe, its height is 1.4 meters and its inner diameter is 60 mms with constant scale division at the top and bottom. The pipe is covered with an end cap. The particles are dropped into the pipe through a 6-mm concentric inlet hole with $v_0 \cong 0$ initial velocity. Paraffin was used as measuring liquid; the advantage of it is that fertilizers - which have chemically salt components - are less soluble in it than in the water and due to its lower density, lighter particles can also be investigated (e.g. plant seeds).

I examined 15-20 particles of each fertilizer. Firstly, for every particle, I determined three dimensions perpendicular to each other and their mass, and then I stated the floating velocity by putting them one after each other into the airflow of the vertical air channel. Afterwards I dropped the same particles into the liquid descent pipe one at a time and with a stopwatch measured the time during which they take the distance between the top and bottom sign.



Figure 2. Liquid descent pipe instrument

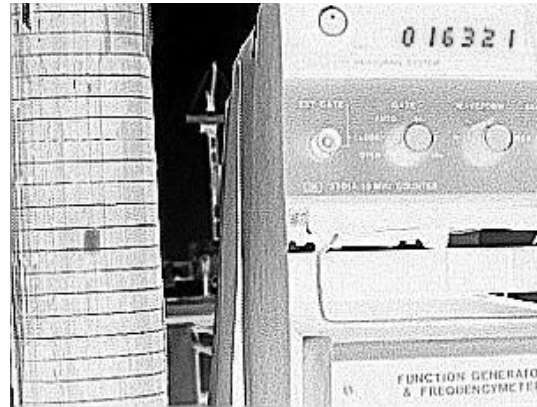


Figure 3. Sinking fertilizer particle in the middle of the descent pipe (left side), signal generator and counter (right side)

At the same time, I took sequence photographs of the particle movement in the middle part of the descent pipe (**Fig. 3.**). Next to the descent pipe, I also placed a set including a test oscillator and a counter that served to measure time accurately. Besides measuring average velocity with digital camera and stopwatch, I compared the results of stopwatch and traditional air channel measurement by solving the equation of motion.

Theoretical aspects of liquid descent pipe

In the descent pipe filled with paraffin the particle is affected by gravity, buoyant force and changing drag effect. The equation of motion can be formulated in the way below according to Newton's second law:

$$m \frac{d^2 y}{dt^2} + C_D A \frac{1}{2} \rho_p \left(\frac{dy}{dt} \right)^2 = mg \frac{\rho_m - \rho_p}{\rho_m}$$

$$K_p = \frac{1}{2} \frac{C_D A \rho_p}{m}$$

where: ρ_p : density of paraffin [kg/m^3]
 ρ_m : density of the fertilizer [kg/m^3]
 m : particle mass [kg]
 g : gravitational constant [m/s^2]
 A : cross section of particle perpendicular to the direction of movement [m^2]
 C_D : drag coefficient
 K_p : resistance coefficient in paraffin [m^{-1}]

The general solution of quadric difference equation with C_1 and C_2 integral constants extending Grift's (1997) solution is the following:

$$y(t) = \frac{1}{K_p} \left\{ \ln \left[\cosh \left((t - C_1) \sqrt{gK_p \frac{\rho_m - \rho_p}{\rho_m}} \right) \right] \right\} + C_2$$

(If the particle starts from 0 height at 0 velocity, then $C_1 = 0$ and $C_2 = 0$)

Knowing the time measured (t) and distance taken I solved the equation numerically to K_p . If the values of C_D drag coefficient are identical for the measuring conditions of the two mediums, k_1 air resistance coefficient is derived based on K_p (ρ_l : air density):

$$k_1 = mK_p \frac{\rho_l}{\rho_p}$$

Knowing v_T average velocity that can be measured easily with a stopwatch:

$$k_1 = K_l m = \frac{mg}{v_T^2} \left(\frac{\rho_m}{\rho_p} - 1 \right) \frac{\rho_l}{\rho_m} \quad \text{Re} = d v \rho_p / \eta_p$$

Using the equation of motion I calculated the theoretical deviations between Grift's aero- and the paraffin descent pipe methods for fertilizer particles of known physical properties. For a 'typical' fertilizer particle ($d \approx 4$ mm) in the case of paraffin descent pipe (paraffin density $\rho_p = 793$ kg/m^3 , viscosity $\eta_p = 2.14 \cdot 10^{-3}$ Pa s) the Reynolds number⁶ is already over 50 after passing the first 0.1-0.2 cms and reaches its value around 500 after taking 3-5 cms distance when the velocity of sinking becomes nearly constant. In the case of the air descent pipe however, the particle velocity, the Reynolds number and consequently, the C_D value changes during the 16 meters fall of the particle.

⁶ GRIFT, T. E., WALKER, J. T. & HOFSTEE, J. W. (1997). *Transactions of the Asae* **40**, 13-20.

Experimental results obtained with the paraffin descent pipe method

I used the low/middle region region of the sinking tube (60 to to 85 cm from the top) for taking pictures. The resistance factors obtained in paraffin were transformed to air resistance factors according to the equations above. **Fig. 4.** compares the average k_1 air drag values measured on 15-20 particles per fertilizer. It can be seen clearly that the photographic and the stopwatch measurements with exact evaluation coincide the best. In **Fig. 5.** in the case of Linz salt, I demonstrate the two kinds of evaluation for each particle as well. The approximate evaluation of stopwatch measurements always gives higher air drag values since it underestimates the average velocity. The elutriation results deviate both in positive and negative direction from the two methods supposed to be the best.

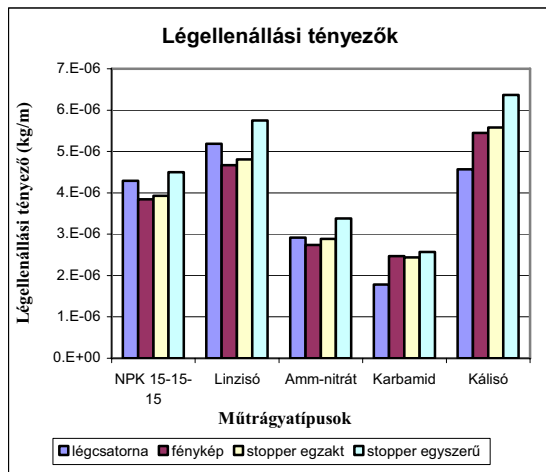


Figure 4. Average air-resistance coefficients of fertilizers measured with different methods

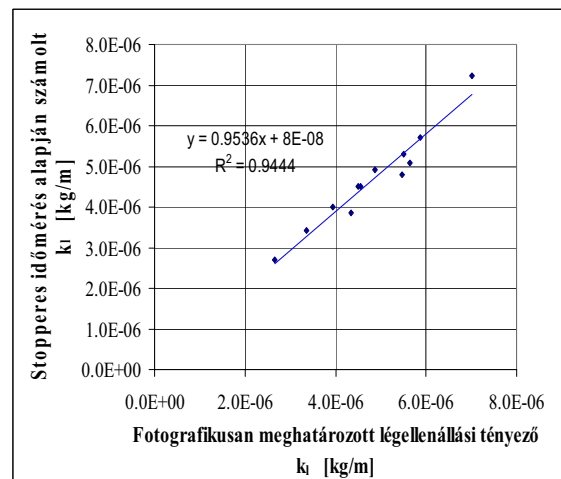


Figure 5. Air-resistance coefficients of the particles of the salt of Linz as compared the values obtained by digital camera and stopwatch method

Conclusions drawn from the results with the descent pipe method

The air drag data measured earlier in air channel on samples of 250 particles different from these were higher in each case except for the carbamide. Hofstee (1992) also found that the floating velocity measured with elutriation can be significantly lower than the value stated with air descent pipe, i.e. the air channel measurement overestimates the value of air drag coefficient. Hofstee explained it saying that the Pitot-tube sensor of the vertical air channel does not measure the actual floating velocity. On the other hand, the flipping, plunging movement of particles also increases the virtual value of the air drag coefficient.

Liquid descent pipe measurements are especially attractive due to their simplicity and the possibility of evaluation without neglect. Further advantage of the appliance is that it is cheap, small, does not require calibration, the measurements are documented with photographs. My tests revealed that methods applying stopwatch and digital camera on identical samples show similar values while the scatter of air channel measurements executed on the same samples is higher. It seems possible to develop the instrument into semiautomatic laboratory appliance for controlling production technology.

4. MAIN FINDINGS OF THE THESIS

4.1. Water-content, particle composition, density and porosity of fertilizers

It can be stated for each type that after production the water-content of fertilizers stored in bags is not significant: varies from 0.05% (potash) to 1.25% (NPK). Water-content can increase during storage, which has unfavourable effect on the texture, ease of handling and spreading of the bulk fertilizer. I found that in cases of NPK-15-15-15 in largest amount the particles fall in the size scale of 2.5-4.0 mm and with salt of Linz 4.0-6.3 mm. It has favourable effect on working width. Carbamide contains in largest proportion the smallest size of 1.0-2.0 mm particle fraction.

According to data gained with different density measurement methods carbamide has the lowest density (1244 kg/m^3) while the other four fertilizers have density similar to each other ($1720 \pm 100 \text{ kg/m}^3$). I found that densities measured with different methods show acceptable agreement and due to literature information ρ_s 'real' density can exceed ρ_g 'virtual' particle density by 10% at most on the average. Therefore, for further ballistic calculations, I used the ρ_s density data - obtained by the air picnometer - considering that it is the closest to the conditions of movement in the air and the expected difference cannot be significant either. I also determined the examined fertilizers' values of volume mass and porosity derivable from it. The volume mass of carbamide is the lowest that is why it requires the largest capacity for storage and transport. On the other hand, probably the high volume mass value of potash can be attributed to the irregular shape. The total Φ_t porosity of NPK 15-15-15 fertilizer is the lowest. Porosities are fairly common: their values vary on the scale of 0.4-0.45, in accordance with my calculated 0.52 theoretical upper limit derived from a simple model. Porosity is decreased by the variation in particle size.

4.2. Surface sliding and friction

According to my experience, at smaller loads – depending on surface and fertilizer - the measured frictional coefficient may increase, decrease or be nearly constant. However, at higher loads, a nearly constant coefficient is observed. Therefore, I regarded the average of the value given at the three largest loads to be the value of friction factor (method “a”). Frictional factors were also determined as a function of displacement (method “b”) in a way that I fitted the applied towing force as a function of the loads for a given displacement. The maximum towing force obtained from the fit was divided by the appropriate normal loading force. The frictional factors obtained this way were averaged for all displacements excluding the first and last values. The averages obtained by method “a” or “b” agreed within error limits. In **Fig. 6. and 7.** the friction force and the friction factors are demonstrated in relation to loading and displacement. In the case of stainless steel - which is an essential structural material – I found that the surface friction factors fall into the range of 0.2-0.35 depending on the type of fertilizer. The friction is the lowest on slippery Teflon surface whereas it is the highest on black steel. The surface friction values that I measured fell into the bottom scale of the data given in literature (0.2-0.7).

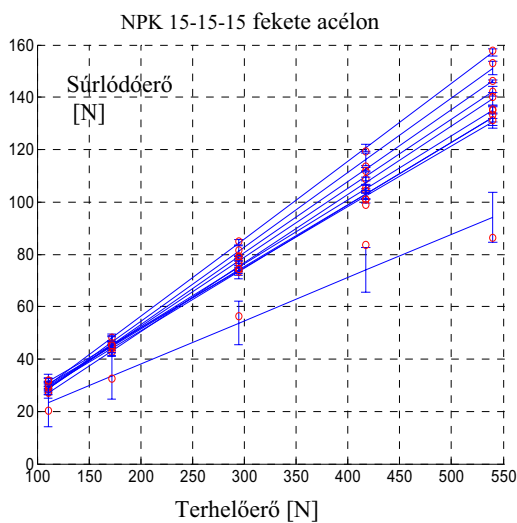


Figure 6. Frictional force between NPK 15-15-15 and black steel fitted as a function of the load

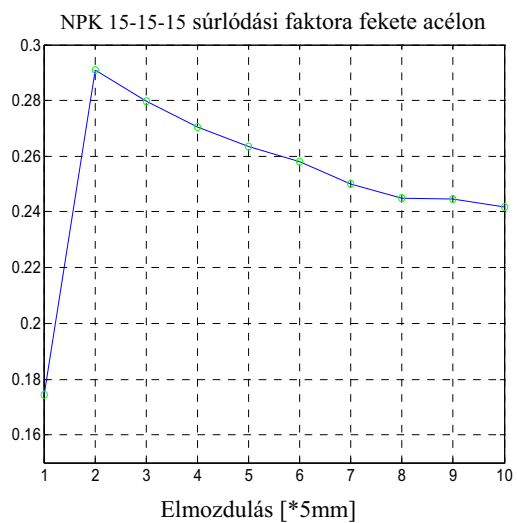


Figure 7. Frictional factor between NPK 15-15-15 and black steel as a function of displacement

4.3. Inner friction

I measured inner friction with the same instrument as the surface frictions but implemented with accessories necessary for rotary type of measurements. The inner friction of potash was

the highest (0.62), and for the ammonium nitrate and carbamide were the lowest (0.40-0.41). I found that μ_i values received from dynamic repose are always 0.1-0.2 higher than the data measured with the shear apparatus. Sitkei also highlights that the two values are dependent of each other and mentions that their values are equal only in extreme cases. The measured angles of repose may depend on the applied equipment: in our case sudden sliding cannot be excluded, while usual dynamic or static ‘natural’ repose appliances provide the angle valid only for the specific conditions of the given experimental method.

4.4. Physical properties of fertilizers particles and their statistical characterisation

By treating some measured parameters or their logarithm as aleatory variable, I checked some hypothesis tests concerning their distribution. After examining the ‘d’ average of the three vertical dimensions I realised that the normal distribution can only be ruled out in the case of ammonium nitrate. The ‘d’ particle size is the smallest for carbamide and largest for the salt of Linz. The order of ‘corresponding’ particle radius is the same as that of the particle size. Furthermore, the $d \approx 2r$ correlation is approximately fulfilled, especially for the nearly spherical particles. Ball shape is the worst with potash whereas it is the best with carbamide; for the other fertilizers the value is over 0.9 (this value is one for a perfect sphere). The particle mass is the lowest with the carbamide due to its small size, but it is also a lot lower at ammonium nitrate than at the other three fertilizers. The mass distribution is lognormal only in the case of NPK 15-15-15 (Fig. 8 and 9), the ammonium nitrate and the potash are not lognormal for sure while the others are ambiguous. I revealed that the density per particle has

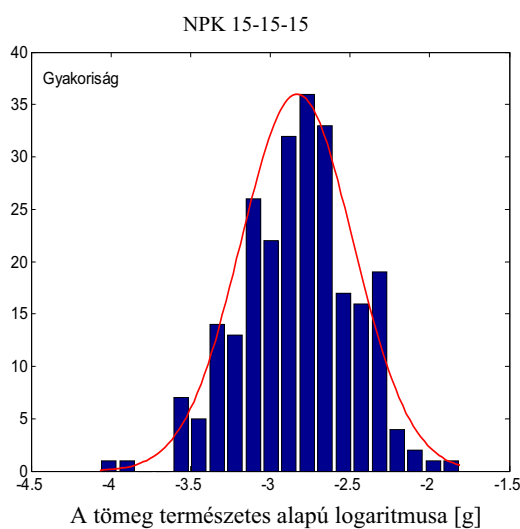


Figure 8. NPK 15-15-15 mass distribution

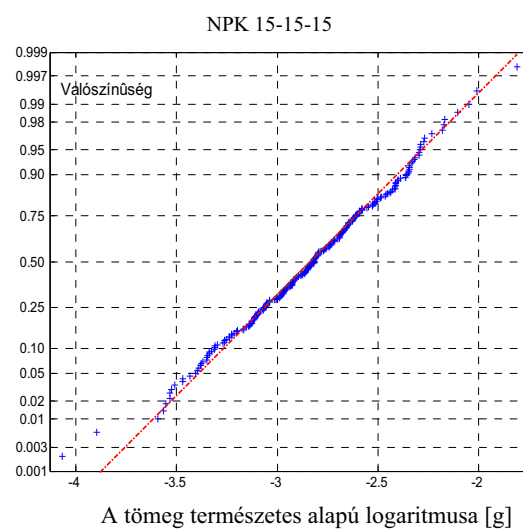


Figure 9. Test of the normal distribution for the mass histogram of NPK 15-15-15

lognormal distribution only at the potash, the NPK 15-15-15 and salt of Linz are uncertain. The density of particles is the most homogeneous in the case of carbamide (5.9% inhomogeneity) whereas it is the least homogeneous at the potash (12.6%). (Of course, the homogeneity of particle density also depends on the accuracy of size specification.) Again, the air resistance factors of potash show obviously normal distribution; not all the others do for sure. In **Fig. 10. and 11.** in pairs, I demonstrate the distribution picture of air resistance coefficients. The considerable difference between the air drag of NPK 15-15-15 and potash can be seen clearly: the latter has less favourable aerodynamic properties. The air drag for potash is the largest and its C_D drag coefficient is significantly high. These features can probably be attributed to the rather irregular crystal shape. The average C_D shape factors derived from average radius or particle sizes coincide fairly well, again, with the exception of potash. In this work, I also made the ballistic calculations for each particle and the results received there suggest that during spreading, the irregularities found in statistical distributions may be inherited in the picture of spreading but the process of spreading can wash the wider differences.

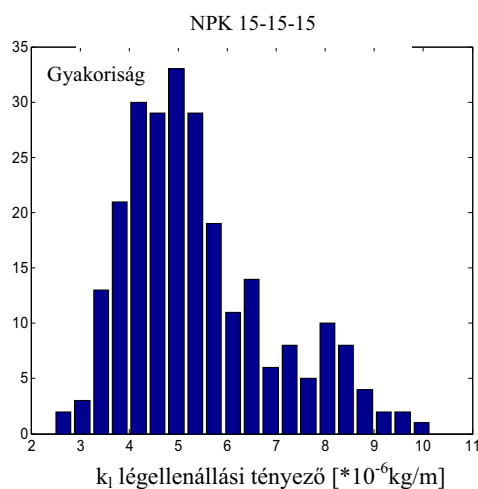


Figure 10. Distribution of air resistance coefficients for NPK 15-15-15

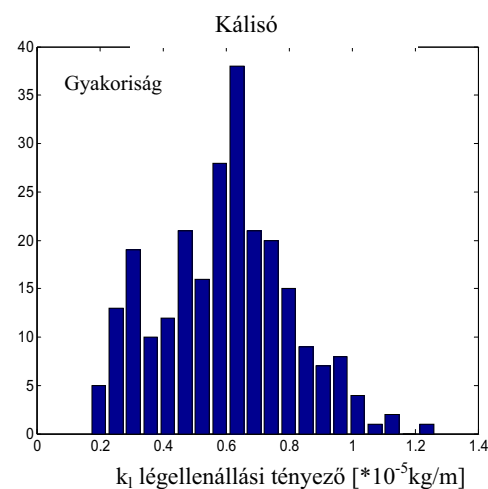


Figure 11. Distribution of air resistance coefficients for potash

4.5. Ballistic calculations

T. Kármán analysed the ballistic problem in detail while P. Soós and his colleagues took part in the elaboration of national agricultural applications. Here I will only give the correlations that I have applied.

$$k_1 = m g / v_t^2$$

$$k_1 = C_D A \rho_l / 2$$

$$m_c = m(\rho - \rho_l) / \rho$$

where k_1 is the air resistance coefficient and C_D is the dimensionless drag coefficient, v_t is the theoretical terminal velocity, 'A' is the largest cross-section of the particle and ' ρ_1 ' is the air density. If the aerostatic pressure is not negligible, Archimedes law can be applied and particle mass 'm' can be replaced with ' m_c ' corrected due to the buoyancy. If the particle is described with \mathbf{v} vector of velocity at a certain point of its trajectory and its β angle closed with the horizontal x-axis, the equation of motion is the following:

$$dv/d\beta = v \operatorname{tg} \beta - k_1 v^3 / (mg \cos \beta)$$

For \mathbf{v} , it is a linear differential equation as function of β , which I solved numerically. Thus, we get the value of velocity with function of β , which I call *velograph*. (The usual hodograph orders the v_x and v_y vertical velocity components to each other.) The dimensional equation system of the trajectory written correctly:

$$x = v_o^2 / g \int f(\beta)^2 / \cos^2 \beta d\beta \qquad y = v_o^2 / g \int f(\beta)^2 / \cos^3 \beta \sin \beta d\beta$$

$$f(\beta) = \{ 1 + k_1 (v_o \cos \alpha)^2 / (mg) [\ln(\cos \alpha (1 + \sin \beta) / (\cos \beta (1 + \sin \alpha))) + \sin \beta / \cos^2 \beta - \sin \alpha / \cos^2 \alpha] \}^{-1/2}$$

The hodographs demonstrates well (**Fig. 12**) that using the average parameters of NPK 15-15-15 fertilizer ($\alpha = -9^\circ$ discharge angle is negative upwards, $v_o = 3 - 25$ m/s, $C_D = 0.69$, $r = 2$ mm) we get 10.6 m/s final velocity for the average particles. At $v_x = 0$, the theoretical terminal velocity $v_T = v_y$ can be read from the hodograph, when after a long time the particle is already descending nearly vertically. Certainly it does not depend on the initial conditions, thus not on the initial velocity either.

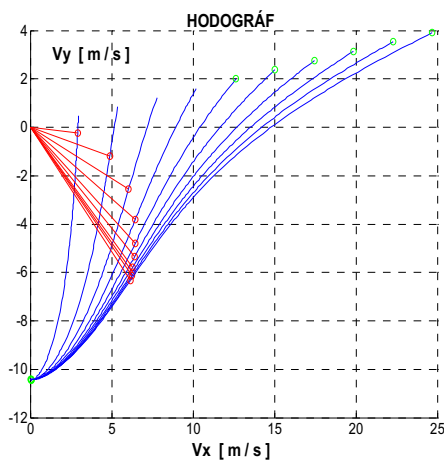


Figure 12. 'Hodograph' of NPK 15-15-15 particles

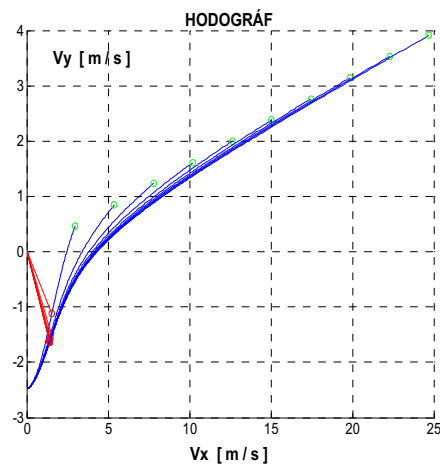


Figure 13. 'Hodograph' of light particles

The hodographs of a light particle are interesting (**Fig. 13.**). I calculated it with values identical with the dimensions of Fig. 12., except for the particle density that is 100 kg/m^3 this

time. For a light particle like these hodographs hardly depend on the initial velocities and, the terminal velocity is only 2.4 m/s .

The disc of spinning disc fertilizer spreader distributes the fertilizer in ring shape. The distribution measured in the radial cross-section of this ring can be calculated from the trajectories (Fig. 14. and 15.) obtained by integrating x, y parametric equations according to β . We get the histograms typical for the cross-section of spreading pattern directly from the trajectories. The most apparent difference is the

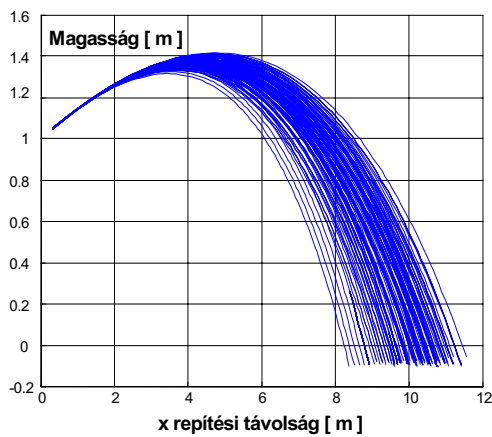


Figure 14. Calculated flight trajectories of NPK 15-15-15 particles

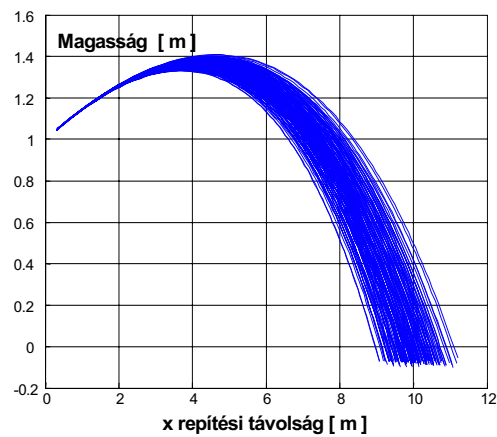


Figure 15. Calculated flight trajectories of 'Salt of Linz' particles

unevenness and asymmetry of the radial section of this ring of spreading for the NPK 15-15-15 fertilizer (Fig. 16.), which covers almost 3 meters range compared to the range of Linz salt that is slightly wider than 2 meters (Fig. 17.). Likely explanation

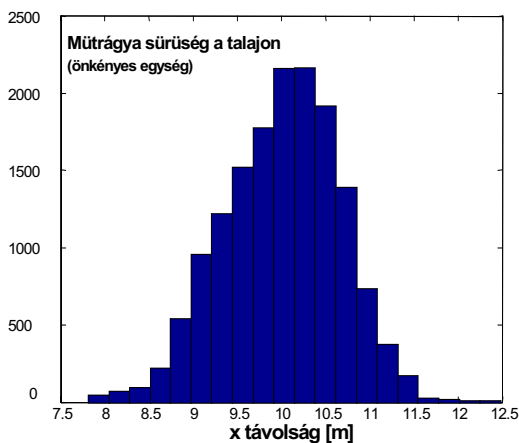


Figure 16. Radial cross-section of spreading ring for NPK 15-15-15 particles

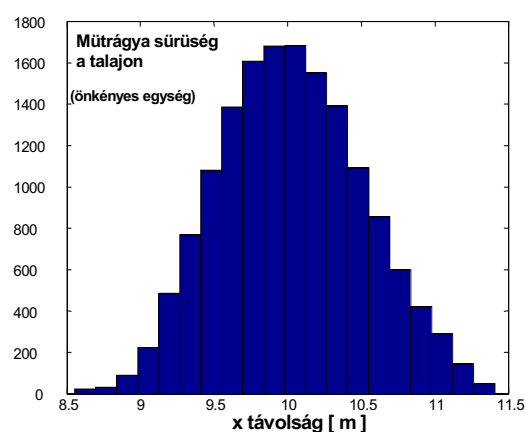


Figure 17. Radial cross-section of spreading ring for 'Salt of Linz' particles

of this is the different physical properties of Linz salt particles. The complex technology of composite fertilizer results in higher spreading uncertainty. At the same time, the most likely distance of radial spreading is about 10 meters for both fertilizers. If we spread light material (100 kg/ m^3) (**Fig. 18.**) and all other parameters remain unchanged, the average casting distance is merely about 1.9 meters. According to my calculations (**Fig. 19.**), raising the discharge velocity from 10 to 20 m/s results in an increase of casting distance by 5 meters, while the rise from 60 to 70 m/s only adds 1.9 meters. In accordance with experience, I conclude that raising the discharge velocity does not increase the casting distance proportionally. I made simulations for the change of α discharge angle and H disc position too. I revealed that changing these parameters would not result in reasonable improvement in increasing casting distance compared to usual constructions.

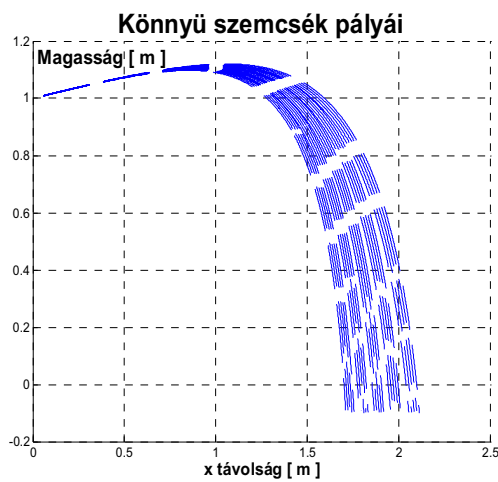


Figure 18. Calculated flight trajectories of light particles

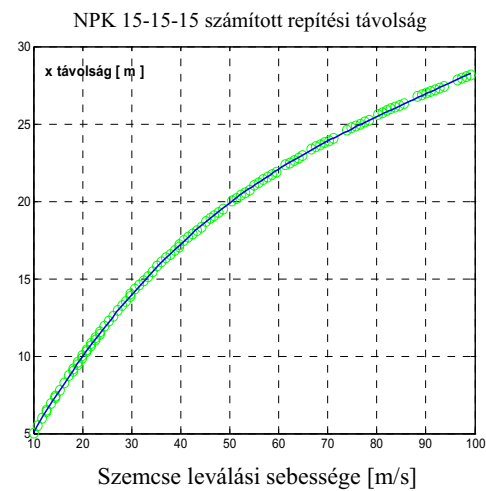


Figure 19. Calculated casting distance of the average NPK 15-15-15 particle as a function of discharge velocity

Calculation of the full spreading pattern

By using the former radial histograms as input data, the full spreading pattern on the arable land can be calculated. To this end, two subsequent geometric transformations must be executed. First I imitate the rotation of the disc into by rotating the initial histogram with $\Phi = 0-90^\circ$ incremented angle. Thus, I get one quarter of the whole ring. Then I multiply the received quarter ring points by small, y-direction shifts that represent the movement of the tractor. The new co-ordinates of the points multiplied by rotation and shift give the co-ordinates of particles landing on the soil (**Fig. 20.**). By making the increments of rotation angle random the operation of the real spinning disc can be 'imitated'. Because of symmetry, it is sufficient to calculate the pattern on the right. Here the tractor speed is neglected

compared to the velocity of discharging particles. **Fig. 21.** shows the spreading pattern vertical to the y direction of movement. It is similar to the early theoretical results and experience: it demonstrates well the unevenness of spreading known about spinning disc fertilizer spreader. Comparing the spreading patterns I found that spreading of the compound NPK 15-15-15 fertilizer is somewhat less even than that of the Linz salt.

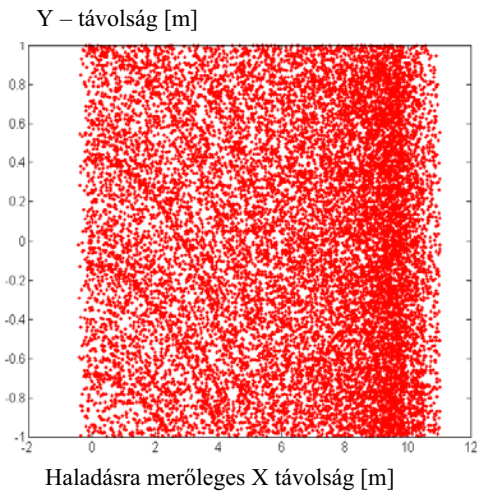


Figure 20. Spreading pattern of the 'Salt of Linz' particles on the arable land ($\Phi = 0-90^\circ$)

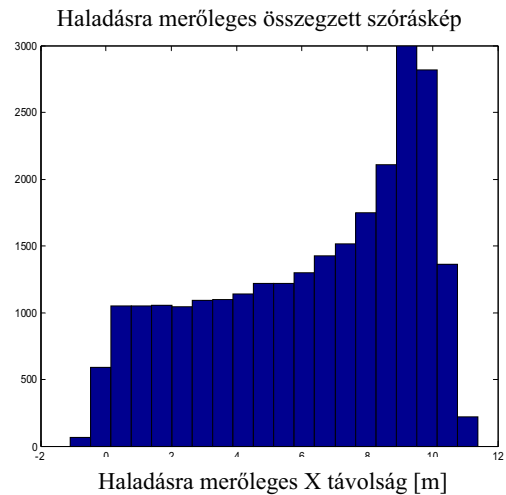


Figure 21. Spreading pattern of the 'Salt of Linz' particles perpendicular to the movement of the tractor ($\Phi = 0-90^\circ$)

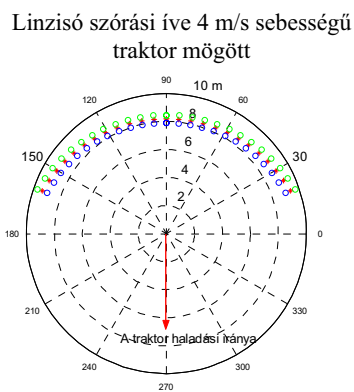


Figure 22. Initial spreading ring of the 'Salt of Linz' particles behind the tractor ($\Phi = 30-150^\circ$)

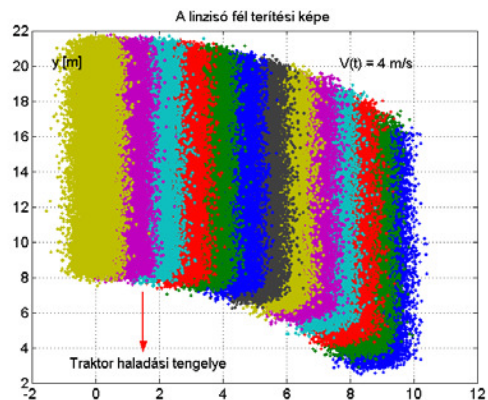


Figure 23. Spreading pattern of the 'Salt of Linz' particles behind the tractor after some time ($\Phi = 30-150^\circ$)

I treated the effect of the tractor's v_t velocity by changing the frame of reference to land coordinate system using the following transformations:

$v_y = v_o \cos\alpha \sin\beta - v_t$ $v_x = v_o \cos\alpha \cos\beta$ and the new direction of casting is $\text{tg } \gamma = v_y/v_x$.
 Its graphic demonstration can be seen in **Figure 22-23**. From the numeric evaluation of unevenness of spreading, I revealed that the advancement of the tractor at the usual (4 m/s) speed has negligible effect on the evenness of spreading vertical to the advancement. Theoretically, the extent of unevenness of spreading can be reduced if the particle flow of the disc is at the maximum in the direction of movement. **Figures 24-27** represents the findings of such an 'experiment', and clearly shows the beneficial effect of the weighted particle flow in the direction of movement.

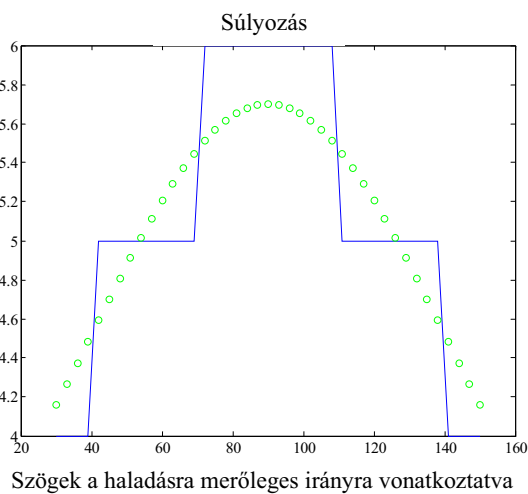


Figure 24. Theoretical weight function for improving the spreading quality of carbamide ($\Phi = 30\text{-}150^\circ$)

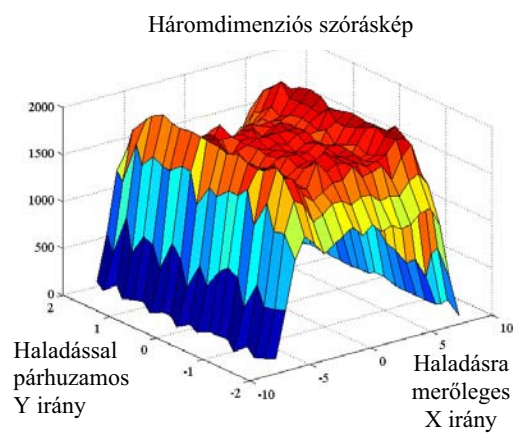


Figure 25. 3D spreading pattern of carbamide after application of the weight function shown in Fig. 23.

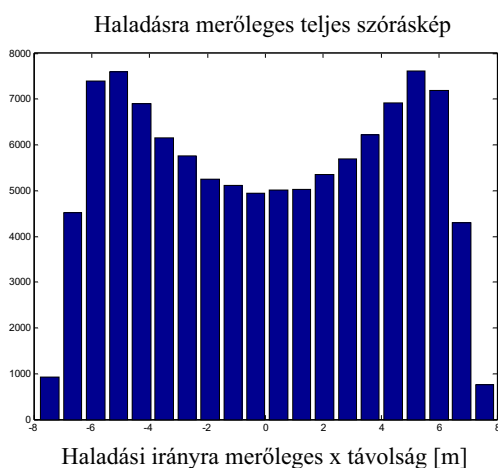


Figure 26. Usual spreading pattern of carbamide, perpendicular to the direction of the movement of the tractor

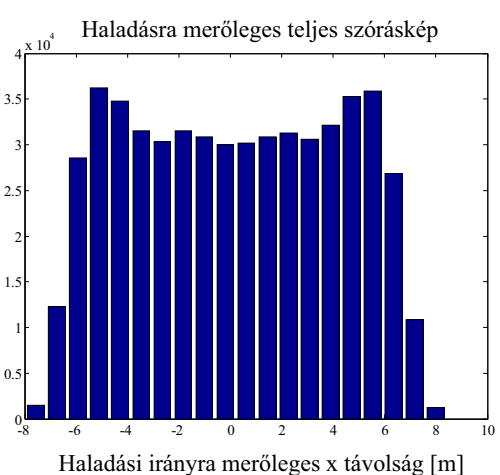


Figure 27. Spreading pattern of carbamide, after improving by the weight function shown in Fig. 23

I measured the physical properties useful for predicting the spreading pattern of five different fertilizers, and the results are summarised in **Table 1**. To calculate the spreading pattern I chose the simplest (isotope) model in which the particle flow leaving the disc is even in every allowed direction. Compared to discs in use the isotope model emphasises spreading to the edges. In spite of this simplistic view, the results are in accordance with certain empirical facts, and the differences between the characteristics of spreading disclose the most sensitive parameters. For instance, it is clear that the carbamide particles do not fly far due to their small size and low density while the reason for the shorter trajectory of potash is its bad aerodynamic properties. Although NPK 15-15-15 and potash fly to similar distance, the compound NPK 15-15-15 can be spread less evenly. Comparing the different fertilizers I found that the C_D drag coefficient is a linear function of the ball shape factor, ($R^2 = 0.90$) whereas the distance of casting is increasing with the weight of the particle.

Table 1.

Fertilizer	NPK 15-15-15	Salt of Linz	Carb- amide	Ammoni- um nitrate	Potash
d- size [mm]	3.97 ± 0.47	4.25 ± 0.63	2.39 ± 0.29	3.08 ± 0.67	3.83 ± 0.56
mass [mg]	62.6 ± 22.1	67.7 ± 28.6	9.55 ± 3.31	28.2 ± 16.2	45.7 ± 17.3
density [kg/m ³]	1758 ± 146	1676 ± 132	1244 ± 73	1611 ± 103	1840 ± 231
ball - shape	0.91 ± 0.06	0.90 ± 0.06	0.96 ± 0.02	0.92 ± 0.04	0.78 ± 0.07
air-resistance coefficient [10 ⁻⁶ kg/m]	5.4 ± 1.5	5.8 ± 2.0	1.7 ± 0.4	3.2 ± 1.5	6.0 ± 2.1
drag coefficient (C_D)	0.69 ± 0.08	0.63 ± 0.06	0.59 ± 0.04	0.63 ± 0.06	0.80 ± 0.12
casting distance [m]	10.0 ± 0.7	10.0 ± 0.5	7.4 ± 0.6	9.0 ± 0.6	8.5 ± 0.5

One of the most interesting observations is that assuming identical initial velocities the average casting distance is a linear function of the inverse of the average particle radius ($R^2 = 0.99$) if we omit potash with its very irregular shape (**Fig. 28.**). If I fit the predicted casting distance for 1000 particles (**Fig. 29.**) of four types of fertilizers as a function of $1/r$ gives $R^2 = 0.86$ regression coefficient. The close relationship – which, in addition, does not depend on the type of fertilizer in the case of four fertilizers either – may be in accord with the fact that the particle surface area / weight ratio is proportional to $\approx 1/r$ in case of particles with similar density. In the $1/r$ relation, the sail effect factor (K_v) plays an important role as K_v is proportional to the surface/volume ($\approx 1/r$) ratio and it is known from the equation of motion that the air drag is proportional to the sail effect factor and the square of the velocity. The

approximate equation valid for horizontal casting lends further support to the validity of the $1/r$ rule. I calculated the expected distance of casting in the extreme range of 0.1-4 mm particle radius using

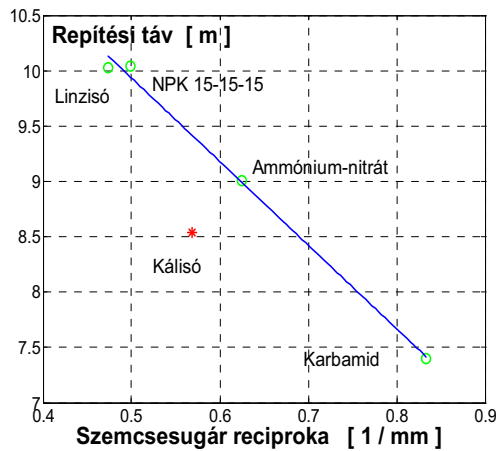


Figure 28. Average of the predicted casting distances for the five different fertilizers

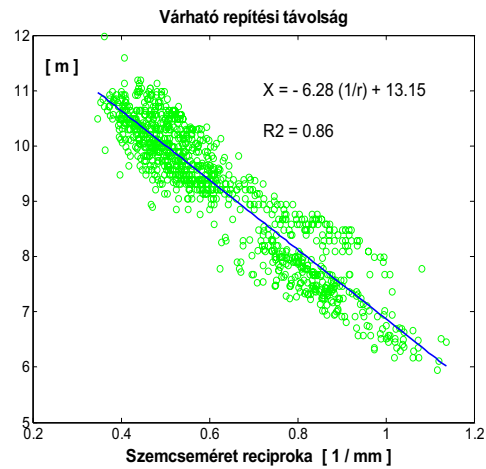


Figure 29. Theoretical casting distance as a function of the particle radius

the usual parameters ($\alpha = -9^\circ$) of NPK 15-15-15. I revealed that for the typical 1-3 mm range of particle radius the distance of casting is linear as a function of $1/r$ or it can be fit with a mild quadratic function. If we fit it as a function of $\ln(1/r)$, the quadratic fit gives good approach for the whole 0.1-4 mm range. The $1/r$ rule is encouraging since the size and velocity of particles may be measured during spreading. Hence, the method may be suitable for immediate prediction of spreading pattern – without ballistic calculations. Grift and Hofstee suggested a similar method in 2002. They calculated the 'landing matrix' in advance and got the impact points from interpolation instead of solving the ballistic problem for each particle.

5. NEW FINDINGS OF THE THESIS

1. I elaborated a complex method for measuring the physical properties of a large number of fertilizer particles. The total porosities of particle clusters were determined from their real volumes using my improved dry-pycnometer method. I derived the theoretical upper limit of total porosity from a geometric model and found that all experimental values were indeed smaller. I determined the density per particle using the particle's perpendicular dimensions.

2. I introduced a new, paraffin filled descent pipe method for indirect measurement of the air resistance coefficients of particles. I found that the aerodynamic data obtained with the new tool are more reliable than those obtained by floating in vertical air channels. However, the similarity of the air resistance coefficients obtained with two different methods experimentally supports the adequacy of the new method. The parameters determined this way are useful for the approximate calculation of the ballistic path and the impact points.
3. I developed a simulation program called 'virtual fertilizer spreader' that is capable to compute the trajectories and impact points of many fertilizer particles in the air from the initial conditions of sloped casting.
 - 3.a. As an alternative of the 'hodograph' visualisation $v_y = f(v_x)$ of velocity components I introduced the 'velograph' ($v = f(\beta)$, the magnitude of velocity as a function of it's direction) that displays the velocity range on the whole path. Using this representation, I proved theoretically that in the case of spherical particles C_D is constant within $\pm 3\%$ on the path. Hence, for particles similar to ball shape, an effective, constant C_D may be used for the calculation of impact points.
 - 3.b. I determined the expected casting distances of the fertilizers as a function of discharge velocity, discharge angle and disc position. I conclude that not much gain can be obtained from the adjustment of these parameters with respect to commercial spreading machines.
4. To process the impact points obtained from ballistics I developed the second task of the '*virtual fertilizer spreader*': prediction of the spreading pattern on arable land. This way the spreading pattern behind the moving machine, the transversal and longitudinal cross-sections of the pattern can be calculated, displayed and quantitatively characterized. Based on these calculations I demonstrate the different spreading patterns for the examined fertilizers, the effect of parameter changes and give numerical evidences for justification of the allowed approaches. In particulars:
 - 4.a I calculated the centre of mass of fertilizer clusters at the radial cross-section of the spreading ring, and found shifts by up to 4% towards the

higher distances if compared to those calculations which were based on the number of particles. I conclude that, it is allowed to use the number of particles for the description of spreading patterns.

- 4.b I found that raising the towing speed of the tractor from zero to 4-8 m/s value, increases the unevenness of spreading vertical to the direction of movement merely by 1-2%, so its effect is negligible at first approximation.
 - 4.c I found that the 'theoretical' one-disc fertilizer spreader – supposed that it gives uniform particle flow in the directions behind the tractor- produces the lowest particle density along the axis of movement. I suggest that this 'fault' can be compensated with a disc construction that provides higher particle flow in the direction of movement.
5. I conclude that for most of the fertilizers I examined – exception is the potash because of its irregular shape – the casting distance is a linear function of the inverse of the particle size. This finding allows estimation the casting distance for the fertilizers measured on the working machine during operation - without any ballistic calculations.

6. APPLICATION OF THE RESULTS IN PRACTICE

1. The paraffin filled descent pipe allows the investigation of the aerodynamic properties of fertilizers before their usage. The new tool can be further developed to deduce the aerodynamic properties of grain. In general, I suggest the application of the descent pipe method instead of the conventional vertical air channel (elutriator).
2. Automatic density measurement per particle could be made suitable for quality control of fertilizer products.
3. The last two modules of the 'virtual fertilizer spreader' are ready: the ballistic and spreading modules were prepared. Based on the latest theoretical findings the first module simulating the movement of particles on the disc could be developed in the

frame of another project. With the aid of the virtual spreader, the calculated and measured spreading patterns can be compared. Such an efficient tool is invaluable in machine construction and may be applied in education as well.

4. Alternatively, to accomplish site-specific fertilizer distribution, spinning disc devices should be equipped with optical size and velocity sensors. The 'on line' spreading pattern prediction depends on the fertilizer type and machine setting and can be improved by 'neural network' algorithms. Consequently, on board computer/GPS combination would be suitable for the control of the machine, which is capable for site-specific fertilizer spreading.

7. PUBLICATIONS RELATED TO THE THESIS

1. Csizmazia Z. - Balló B. - Kasza F. - Polyák N. I. - Hagymássy Z. - Ancza B. E. – **Gindert-Kele Á.** (2001) Súrlódásmérő készülék fejlesztése. Mezőgazdasági Technika. 42. évf. 7. sz. 4-6. p.
2. Csizmazia Z. - Hagymássy Z. – **Gindert-Kele Á.** - Ancza B.E. (2001) Összetett műtrágya súrlódási viszonyainak vizsgálata. Georgikon Napok. Keszthely. 1136-1139.p.
3. Ancza B.E. - Csizmazia Z. – **Gindert-Kele Á.** - Hagymássy Z. (2002) Műtrágyaszemcsék súrlódása különböző felületeken. Kutatási és Fejlesztési Tanácskozás. Gödöllő. 127-131.p.
4. Hagymássy Z. - Csizmazia Z – **Gindert-Kele Á.** - Ancza B.E. (2002) Műtrágyaszemcsék belső súrlódása. Kutatási és Fejlesztési Tanácskozás. Gödöllő. 160-164.p.
5. **Gindert-Kele Á.** - Csizmazia Z. - Ancza B.E. - Hagymássy Z. (2002) Műtrágyaszemcsék néhány fizikai jellemzője. Kutatási és Fejlesztési Tanácskozás. Gödöllő. 165-169.p.
6. **Gindert-Kele Á.** - Csizmazia Z. - Ancza B.E. - Hagymássy Z. (2002) Műtrágyák fizikai jellemzőinek összehasonlító vizsgálata. Wellmann Oszkár Tudományos Tanácskozás. Hódmezővásárhely. 63.p.
7. Hagymássy Z. - Csizmazia Z - **Gindert-Kele Á.** (2002) Parcella műtrágyaszóró gép fejlesztése. Wellmann Oszkár Tudományos Tanácskozás. Hódmezővásárhely. 64. p.
8. Csizmazia Z.-Ancza B.E. - **Gindert-Kele Á.** -Hagymássy Z. (2002) Internal friction of fertilizers. AgEng International Conference on Agricultural Engineering. Budapest. 170-171. p.
9. **Gindert-Kele Á.** (2002) Összetett műtrágya fizikai jellemzői. EU konform mezőgazdaság és élelmiszerbiztonság Tudományos Konferencia. Debrecen 356-361. p.
10. **Gindert-Kele Á.** - Hagymássy Z. - Ancza B.E. - Csizmazia Z. (2002) Műtrágyák aerodinamikai jellemzőinek vizsgálata. V. Nemzetközi Élelmiszertudományi Konferencia, Szeged 119-120.p.

11. Ancza B.E. - **Gindert-Kele Á.** - Hagymássy Z. - Csizmazia Z. (2002) Műtrágyaszóró gép munkaminőségi jellemzői, V. Nemzetközi Élelmiszertudományi Konferencia. Szeged 147-148. p.
12. Hagymássy Z. - Csizmazia Z. - **Gindert-Kele Á.** - Ancza B.E. (2002) Módosított parcella szórógép vizsgálata, V. Nezetközi Élelmiszertudományi Konferencia. Szeged 125-126. p.
13. E. Ancza - Z. Csizmazia - **A. Gindert-Kele** - Z. Hagymássy (2002) Friction between fertilizer particles and different types of surfaces, Hungarian Agricultural Engineering, No. 15. 41-43. p.
14. **Gindert-Kele Á.** (2003) A pétisó súrlódási jellemzői, Kutatási és Fejlesztési Tanácskozás. Gödöllő. 3. kötet 46-50. p.
15. **Gindert-Kele Á.** (2003) Valós szóráskép jóslása nitrogén és összetett műtrágyák esetén a ballisztikus probléma megoldásával, Mezőgazdasági Technika 4. sz. 2-4.p.
16. **Gindert-Kele Á.** (2003) Predicting fertilizer spreading pattern, Natural Resources and sustainable development Oradea
17. **Á. Gindert-Kele** (2003) Fertiliser pattern prediction of spinning disc spreaders Hungarian Agricultural Research, No. 9. 6-8. p
18. **Gindert-Kele Á.** - Hagymássy Z. - Ancza E. (2004) Műtrágyák szórásképének jóslása a szemcsék vizsgálata alapján Kutatási és Fejlesztési Tanácskozás. Gödöllő. 1. kötet 160-164. p.
19. Hagymássy Z. - **Gindert-Kele Á.** - Ancza E. (2004) Mikroparcella műtrágyaszóró gép vizsgálata Kutatási és Fejlesztési Tanácskozás. Gödöllő. 1. kötet 34-38. p.
20. **Gindert-Kele Á.** (2005) Új mérőeszközök alkalmazása műtrágyaszemcsék vizsgálatára Kutatási és Fejlesztési Tanácskozás. Gödöllő
21. **Gindert-Kele Á.** (2005) Folyadékos ejtőcső fejlesztése műtrágyaszemcsék aerodinamikai jellemzőinek mérésére. Összehasonlítás a légcatornás módszerrel. Mezőgazdasági Technika, 1. sz. 2-4.p.